

pubs.acs.org/JACS Communication

# Adaptable Multivalent Hairy Inorganic Nanoparticles

Caleb A. Bohannon, Andrew J. Chancellor, Michael T. Kelly, Tram T. Le, Lei Zhu, Christopher Y. Li, and Bin Zhao\*



Cite This: J. Am. Chem. Soc. 2021, 143, 16919-16924



**ACCESS** 

Metrics & More





ABSTRACT: We report a polymer brush-based approach for fabricating multivalent patchy nanoparticles (NPs) with the number of nanodomains (valency) from 6 to 10, potentially from 1 to 10, by exploiting the lateral microphase separation of binary mixed homopolymer brushes grafted on NPs with a radius comparable to the polymer sizes. Well-defined mixed brushes were grown on 20.4 nm silica NPs by two-step surface-initiated reversible deactivation radical polymerizations and microphase separated laterally upon casting from a good solvent, producing multivalent NPs on 2D surfaces. A linear relationship between valency and average core size for the corresponding valency was observed. The mixed brush NPs exhibited abilities to form "bonds" through the overlap of nanodomains and to change the valency when interacting with adjacent NPs. This method could open up a new avenue for studying patchy NPs.

Patchy particles are a class of unconventional particles where the surface where the surface is patterned with a small number of discrete, distinct domains. 1-5 These particles, including the simplest version, Janus particles with contrasting properties on the opposite sides of the particles, 6-9 hold promise for many applications. 1-9 They are used as effective Pickering emulsion stabilizers,8 for constructing meta-materials with complex structures that cannot be achieved with particles of uniform surface characteristics, 1,2 and for building colloidal assemblies that mimic organic compounds (colloidal molecules).3 Polymer brushes have emerged as a versatile bottom-up means for fabricating patchy NPs owing to their ability to undergo self-reorganization in response to environmental changes. 4,10-14 Most notably, surface patterning of homopolymer-grafted NPs with relatively low grafting densities was attained upon lowering solvent quality to collapse the uniform brushes into surface-pinned micelles, producing patchy NPs with a small number of domains or helicoidal patterns. 4,10,11 Multicomponent brushes provide greater flexibility toward patchy NPs and assemblies. 12-20 Programmed surface patterning and assembly of diblock copolymer-grafted gold NPs were realized by first formation of patchy NPs through the collapse of the inner block and then self-assembly into small, well-defined clusters. 14 Soft patchy NPs with a polymeric core were made from ABC triblock copolymer micelles by collapsing one of the two outer blocks in the corona and self-assembled into complex well-ordered structures. Despite the progress, it remains a challenge to prepare patchy NPs with a valency from 1 to 10 using polymer brush-grafted NPs (hairy NPs).

Herein we report a method for fabricating patchy NPs with the number of nanodomains (valency) from 6 to 10 (i.e., multivalent NPs<sup>21</sup>), potentially from 1 to 10, without resorting to poor solvents by using binary mixed homopolymer brushgrafted small NPs. These NPs can form "bonds" through the overlap of their nanodomains and change their valency

according to the environment. Mixed brushes, composed of two distinct homopolymers randomly or alternately endtethered on a surface, exhibit intriguing behaviors.  $^{21-32}$  Simulations have shown that for mixed brushes on spherical NPs with a radius comparable to the polymers' unperturbed root-mean-square end-to-end distances ( $R_{\rm rms}$ ), various islanded structures are formed from lateral microphase separation of the two grafted polymers, yielding multivalent NPs with 2 to 12 (except 11) nanodomains. The valency is governed by core size, grafting density ( $\sigma$ ), chain length, etc., among which core size plays a significant role. Moreover, upon assembly, polymer microphase separation competes with NP close packing; both commensurate and incommensurate structures could occur, rendering this type of multivalent particles intrinsically adaptable.

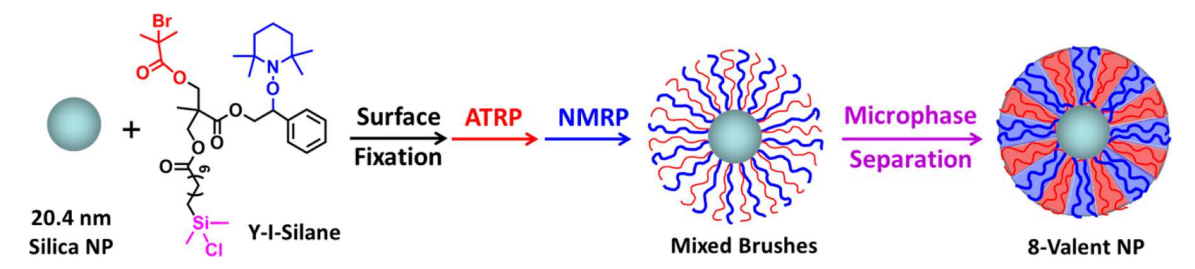
We synthesized mixed poly(tert-butyl acrylate) (PtBA)/polystyrene (PS) brushes on 20.4 nm silica NPs (Scheme 1). A monochlorosilane-terminated asymmetric difunctional initiator (Y-I-Silane), containing one atom transfer radical polymerization (ATRP³³) initiating group and one nitroxide-mediated radical polymerization (NMRP³⁴) initiating moiety, was immobilized onto 20.4 nm silica NPs (see the Supporting Information). The initiator-functionalized NPs were used for growing brushes by sequential surface-initiated ATRP of tertbutyl acrylate at 75 °C and surface-initiated NMRP of styrene at 120 °C, each with the addition of a free initiator. Type A total of nine mixed brush NP samples with a fixed PtBA  $M_{\rm n}$  of 19.6 kDa and various PS  $M_{\rm n}$ s (from 6.1 to 31.5 kDa) were prepared. The calculated PS grafting densities were in the range of 0.27—

Received: August 6, 2021 Published: October 8, 2021





Scheme 1. Synthesis of Binary Mixed Homopolymer Brushes on 20.4 nm Silica NPs and Formation of Multivalent NPs with an 8-Valent NP as an Example



0.49 chains/nm<sup>2</sup>,<sup>37</sup> similar to  $\sigma_{\text{PtBA}}$  (0.37 chains/nm<sup>2</sup>). The PtBA's  $R_{\text{rms}}$  was estimated to be 8.3 nm, while the PS  $R_{\text{rms}}$  values ranged from 5.2 to 11.7 nm,<sup>36,38</sup> comparable to the radius of silica NPs. With increasing PS  $M_{\text{n}}$ , the volume fraction of PS ( $f_{\text{PS}}$ ) increased and became greater than 0.50 at PS  $M_{\text{n}}$  = 20.0 kDa. The characterization data and calculated values are summarized in Table 1.

Table 1. Characterization of Mixed PtBA/PS Brush-Grafted Silica NPs

hairy NPs	PS $M_n$ (kDa), $\tilde{\mathbb{D}}^a$	$\sigma_{ ext{PS}} \left( \begin{array}{c}  ext{chains} / \\  ext{nm}^2 \right)^b$	$\frac{\text{PS } R_{\text{rms}}}{(\text{nm})^c}$	$f_{\mathrm{PS}}^{}d}$
BNP-6.1k	6.1, 1.27	0.45	5.2	0.27
BNP-9.7k	9.7, 1.26	0.37	6.5	0.32
BNP-10.9k	10.9, 1.18	0.33	6.9	0.32
BNP-12.9k	12.9, 1.28	0.32	7.5	0.35
BNP-15.2k	15.2, 1.17	0.27	8.1	0.35
BNP-20.0k	20.0, 1.18	0.39	9.3	0.51
BNP-23.0k	23.0, 1.17	0.37	10.0	0.53
BNP-27.6k	27.6, 1.19	0.40	10.9	0.59
BNP-31.5k	31.5, 1.25	0.40	11.7	0.62

"The number-average molecular weight  $(M_{\rm n})$  and dispersity (D) were determined by size exclusion chromatography (SEC) using PS standards. The  $M_{\rm n}$  and D of PtBA were 19.6 kDa and 1.20, respectively. We previously found that the PtBA  $M_{\rm n}$  from SEC was similar to the  $M_{\rm n}$  determined from the monomer conversion. The  $M_{\rm n}$  determined from the monomer conversion  $M_{\rm n}$  is the backbone C-C bond number, and  $M_{\rm n}$  is the C-C bond length (1.54 Å). The  $M_{\rm n}$  for PtBA was unavailable, and we used PS  $M_{\rm n}$  for estimating PtBA's  $M_{\rm rms}$  giving 8.3 nm. The densities of PtBA (1.008 g/cm³) and PS (1.052 g/cm³) were used in calculating  $M_{\rm PS}$ .

To visualize the NPs' morphologies, transmission electron microscopy (TEM) was performed. The brush NPs were dropcast on carbon-coated TEM grids from CHCl<sub>3</sub> at 0.25 mg/mL<sub>2</sub> annealed with chloroform vapor for >3 h, and stained with RuO<sub>4</sub> for 7 min. RuO<sub>4</sub> selectively stains PS, making it dark under TEM.<sup>36</sup> Figure 1a-j shows TEM micrographs of one PtBA NP without staining and single NPs of nine mixed brush samples. All mixed brushes were microphase separated, yielding spoke-like multivalent NPs with a small number of nanodomains extending outward from the core. The most common valency was 8 except for BNP-6.1k, whose nanodomains were difficult to discern due to the short nanodomains (Figure 1b). The clearest multivalent NPs were found for the samples with PS  $M_n$  from 10.9 to 23.0 kDa (Figure 1d– h). The size of brush NPs and the length of dark nanodomains increased with increasing PS M<sub>n</sub>. The PS domains were somewhat uniform in width when the PS  $M_n$  was  $\leq 15.2$  kDa (~7 nm for BNP-12.9k) but became truncated wedge-like at

PS  $M_n$  = 20.0 kDa.<sup>39</sup> Upon further increasing PS  $M_n$ , the dark domains gradually enclosed the bright nanodomains, and for BNP-27.6k and -31.5k the bright domains were fully covered by PS chains. Note that the degrees of polymerization (DPs) of PS for BNP-27.6k (265) and -31.5k (302) were significantly larger than the PtBA's DP. This is consistent with the simulation result that for asymmetric mixed brushes with a large chain length asymmetry the laterally phase-separated layer is covered with the longer species.<sup>30</sup>

The observed multivalent NPs under TEM are 2D projections; therefore, the valency  $V \sim \frac{r}{r}$ , where r is the NP radius and w is the nanodomain width. Compared with other patchy brush NPs, the valency here arises from the intrinsic lateral microphase separation of mixed brushes and therefore can be tuned by varying parameters such as  $M_{\rm p}$ , f, Flory-Huggins parameter, and  $\sigma$ . Moreover, r plays a significant role, as shown above and by simulations. <sup>31,32</sup> The silica NPs used here exhibited a certain dispersity. To elucidate how the core size affected the valency, BNP-15.2k was stained for 2 min, which made both core NP and PS nanodomains visible under TEM (Figure 1k). We analyzed 102 NPs for core size and valency, and the results are plotted in Figure 1k. A trend was seen that the valency decreased with decreasing core dimension, and each valency corresponded to a size range, which qualitatively agreed with the simulation results.<sup>32</sup> A linear relationship between valency and average core size for each valency was observed (Figure 11), with a slope of 0.42. Extrapolation showed that monovalent (i.e., Janus NPs), divalent, and tetravalent NPs would be obtained from mixed brush NPs with a core diameter of 2.8, 5.2, and 10 nm. Kim et al. studied mixed brush-grafted, ~3 nm gold NPs in toluene by neutron scattering and found that with increasing molecular weights the brush NPs phase separated into Janus NPs. 40 Note that di- and tetravalent NPs could self-assemble into uncommon square lattices.4

These multivalent NPs can interact with each other and form "bonds". Figure 2 shows TEM images of BNP-15.2k, from individual NPs to various-sized clusters and NP lattice. Bonds were formed between NPs via the overlap of nanodomains, much like the  $\sigma$ -bond formation through head-to-head overlap of electron orbitals. The bonded domains were slightly darker and similar in length to unbonded nanodomains (i.e., dangling bonds). In Figure 2c, the formation of two bonds, indicated by arrows, appeared to be in the process. As mentioned earlier, 8 was the most frequent valency of individual NPs, and analysis of 304 hairy NPs showed an average valency of 7.86  $\pm$  0.95. For the lattice (Figure 2l), the most common valency appeared to be 6. Analysis of different-sized assemblies found that the average valency per NP decreased gradually from 7.86  $\pm$  0.95 for

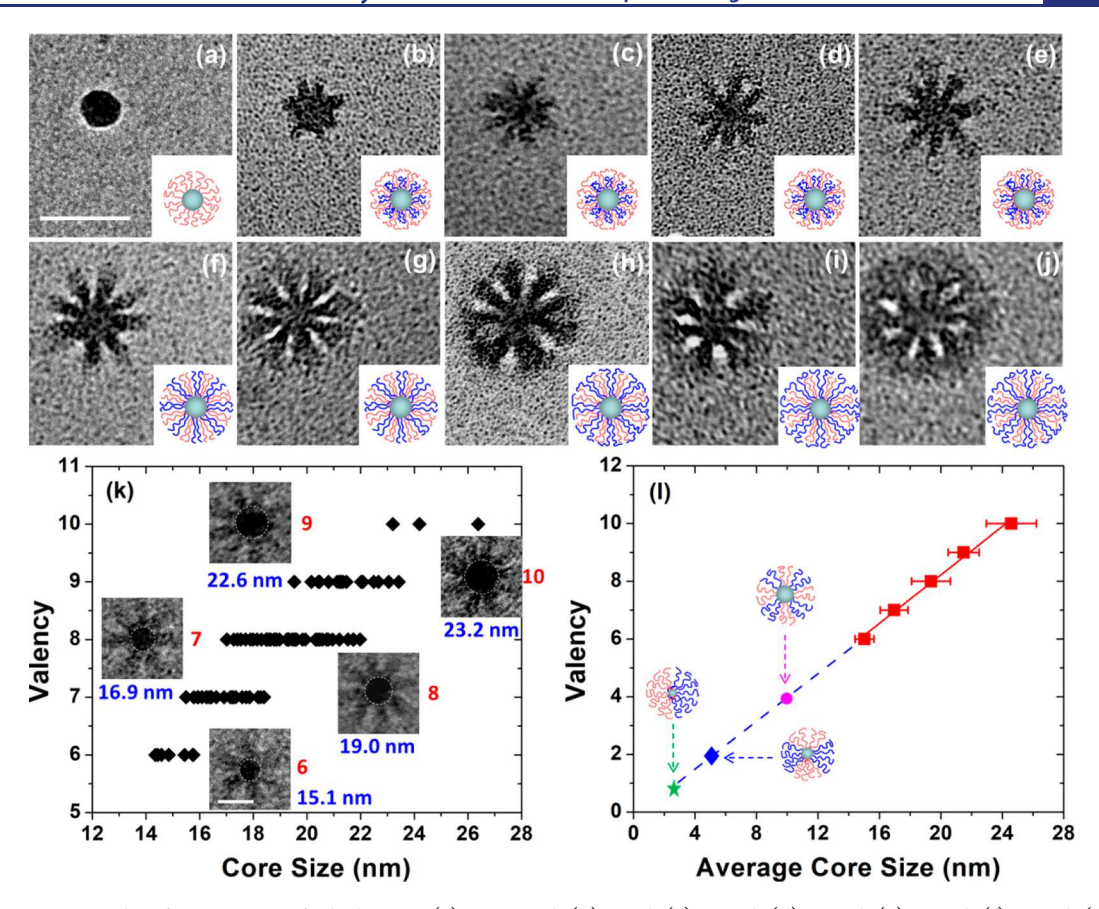


Figure 1. TEM micrographs of one PtBA-grafted silica NP (a), BNP-6.1k (b), -9.7k (c), -10.9k (d), -12.9k (e), -15.2k (f), -20.0k (g), -23.0k (h), -27.6k (i), and -31.5k (j). Scale bar: 50 nm. The mixed brush NPs were stained with  $RuO_4$  for 7 min. (k) Plot of valency vs core size for BNP-15.2k after being stained with  $RuO_4$  for 2 min. Scale bar: 25 nm (see Figure S9 in the Supporting Information for a guided view of nanodomains, where for each multivalent NP dashed lines with a larger circle are drawn). (l) Plot of valency versus average core diameter for the corresponding valency with the standard deviation. The star, diamond, and circle indicate mono-, di-, and tetravalent NPs from extrapolation.

individual NPs to  $7.12 \pm 1.05$  for dimers (212 NPs analyzed),  $6.55 \pm 0.91$  for trimers (123 NPs),  $6.40 \pm 0.91$  for tetramers (156 NPs),  $6.35 \pm 1.00 \text{ for 5-mers} (115 \text{ NPs})$ ,  $6.24 \pm 0.70 \text{ for}$ 6-mers (84 NPs), 6.07  $\pm$  0.79 for 7-mers (126 NPs), 6.09  $\pm$ 0.65 for 8- to 10-mers (150 NPs), and 5.95  $\pm$  0.48 for the lattice (212 NPs) (Figure 2m), indicating that these multivalent NPs were environmentally adaptable. This intriguing observation can be attributed to the competition of two separate self-assembly processes: brush microphase separation, which leads to a finite, NP size-dependent valency for individual NPs, and NP close packing on 2D surfaces, which prefers a hexagonal symmetry. The NP's valency is preserved when it is commensurate with the lattice site's coordination number 6. However, when they are incommensurate, the NP packing dominates the assembly process and the brushes appear to be able to reconfigure their nanodomain sizes to adapt to the lattice, indicating that the lattice's packing requirement could overwrite the core size's effect. It is also possible that the brushes could dictate the packing of smaller NPs. Computer simulations have shown that when the ratio of the spherical core radius (r) to the polymer size  $(R_{rms})$  in the unperturbed state) in the symmetric mixed brush-grafted NPs is <1, the most stable NP packing is simple cubic crystal lattices in 3D and square arrays in 2D (i.e., brushes dominate).<sup>32</sup> At the ratios of r to  $R_{\rm rms} > 1$ , the most stable NP arrangement is body-centered-cubic lattices in 3D and hexagonal arrays in 2D (i.e., core NPs dominate).

Figures 3 and S10 show the TEM micrographs of small and large NP assemblies for nine mixed brush samples, respectively. While the bonds between NPs for BNP-6.1k to -15.2k were formed by dark nanodomains, they changed to bright domains for BNP-20.0k, -23.0k, and -27.6k. This bond inversion was caused by the changes of relative molecular weights and  $f_{PS}$ . When the PS  $M_n$  was  $\geq 20.0$  kDa ( $f_{PS} > 0.50$ ), PtBA became the minority component, forming the bonds between NPs. For BNP-6.1k, the bonds were rather weak due to the short PS chains. On the other hand, for BNP-31.5k, PS was significantly longer than PtBA, making it difficult for PtBA nanodomains to form bonds, as evidenced by the dark gaps between mutually pointing bright nanodomains. Interestingly, the PS bonds in Figure 3e bulged out in the center, while they were straighter in Figure 3b,c, indicating that the PS in BNP-15.2k was more relaxed. Similarly, the PtBA bonds were more flower-like in BNP-20.0k and -23.0k but more uniform in width in BNP-27.6k (Figure \$10).

In summary, we demonstrated the fabrication of multivalent NPs with a valency of 6 to 10 utilizing the spontaneous microphase separation of binary mixed brushes grafted on NPs with a radius similar to the polymer sizes. A linear relationship was observed between valency and average core size. These NPs can form bonds through the overlap of nanodomains, and the valency decreased with increasing NP number in the assembly, showing the NPs' adaptability. Moreover, we observed the bond inversion from one polymer to another

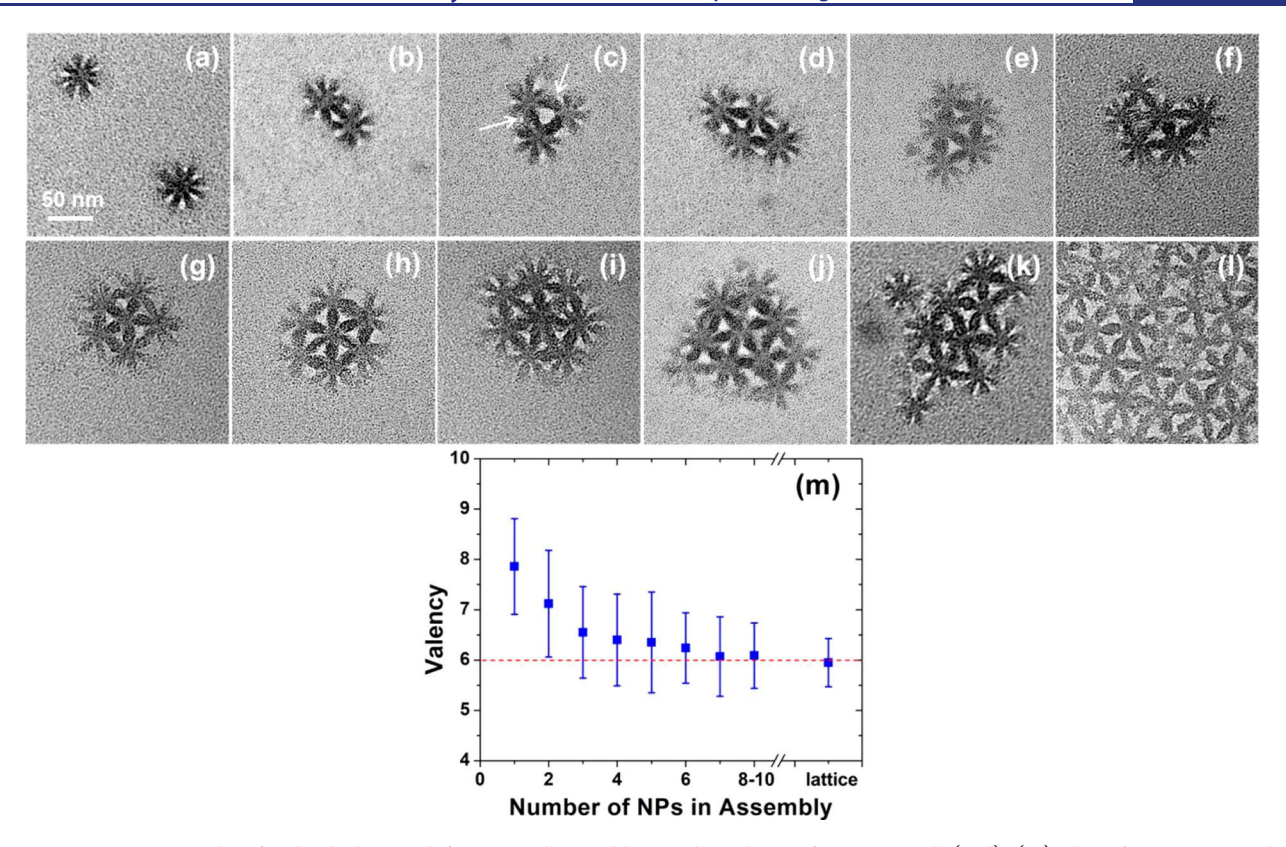


Figure 2. TEM micrographs of individual NPs, different-sized assemblies, and NP lattice for BNP-15.2k (a–l). (m) Plot of average NP valency versus NP number in the assembly.

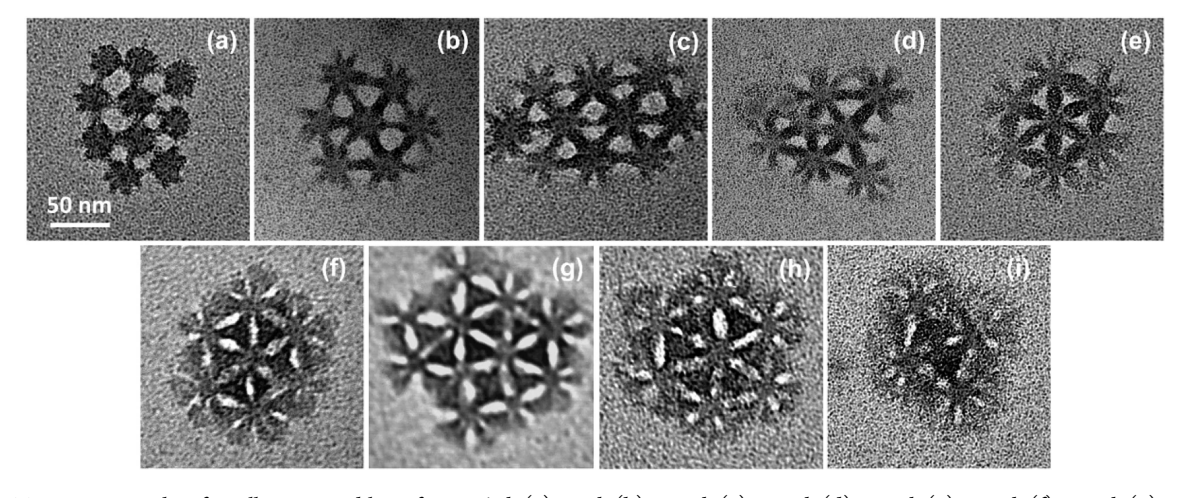


Figure 3. TEM micrographs of small NP assemblies of BNP-6.1k (a), -9.7k (b), -10.9k (c), -12.9k (d), -15.2k (e), -20.0k (f), -23.0k (g), -27.6k (h), and -31.5k (i).

with the change of relative molecular weights of the two polymers. The multivalent NPs presented here were on 2D surfaces (i.e., 2D multivalent NPs). Fox et al. previously observed by cryo-electron tomography that mixed poly(acrylic acid)/polystyrene brushes grafted on 50–90 nm silica NPs phase separated laterally in *N,N*-dimethylformamide. <sup>42</sup> On the other hand, simulation studies showed that mixed brushes in nonselective solvents phase separated laterally over a wide range of solvent conditions when the two polymers were sufficiently immiscible. <sup>21,31,43</sup> Thus, it is feasible to make 3D multivalent NPs from mixed brush-grafted small NPs in solvents. We plan to explore 3D multivalent NPs by using cryo-TEM, selective cross-linking of nanodomains, freeze-

drying, etc. By tuning the core size and brush parameters, multivalent NPs with a valency from 1 to 10 are likely achievable, and thus this bottom-up approach could open up new opportunities for studying patchy NPs, not only in the fabrication but also in the self-assembly behavior in 3D, e.g., by changing the solvent quality, and in 2D, e.g., at the air—water interface by the Langmuir—Blodgett technique.

# ASSOCIATED CONTENT

#### Supporting Information

The Supporting Information is available free of charge at https://pubs.acs.org/doi/10.1021/jacs.1c08261.

Experimental Section; TEM micrographs of large NP assemblies for nine mixed brush NP samples (PDF)

## AUTHOR INFORMATION

# **Corresponding Authors**

Christopher Y. Li — Department of Materials Science and Engineering, Drexel University, Philadelphia, Pennsylvania 19104, United States; ⊚ orcid.org/0000-0003-2431-7099; Email: chrisli@drexel.edu

Bin Zhao — Department of Chemistry, University of Tennessee, Knoxville, Tennessee 37996, United States; ⊙ orcid.org/ 0000-0001-5505-9390; Email: bzhao@utk.edu

#### **Authors**

Caleb A. Bohannon – Department of Chemistry, University of Tennessee, Knoxville, Tennessee 37996, United States

Andrew J. Chancellor – Department of Chemistry, University of Tennessee, Knoxville, Tennessee 37996, United States

Michael T. Kelly – Department of Chemistry, University of Tennessee, Knoxville, Tennessee 37996, United States

Tram T. Le – Department of Chemistry, University of Tennessee, Knoxville, Tennessee 37996, United States

Lei Zhu — Department of Macromolecular Science and Engineering and Department of Chemistry, Case Western Reserve University, Cleveland, Ohio 44106-7202, United States; © orcid.org/0000-0001-6570-9123

Complete contact information is available at: https://pubs.acs.org/10.1021/jacs.1c08261

#### **Author Contributions**

The manuscript was written through contributions of all authors. All authors have given approval to the final version of the manuscript.

## **Author Contributions**

\*C.A.B. and A.J.C. contributed equally.

#### Notes

The authors declare no competing financial interest.

## ACKNOWLEDGMENTS

B.Z. and C.Y.L. thank the NSF for the support (CHE-1709663 for B.Z. and CHE-1709119 for C.Y.L).

#### REFERENCES

- (1) Zhang, Z. L.; Glotzer, S. C. Self-Assembly of Patchy Particles. *Nano Lett.* **2004**, *4*, 1407–1413.
- (2) Chen, Q.; Bae, S. C.; Granick, S. Directed Self-Assembly of a Colloidal Kagome Lattice. *Nature* **2011**, *469*, 381–384.
- (3) Wang, Y. F.; Wang, Y.; Breed, D. R.; Manoharan, V. N.; Feng, L.; Hollingsworth, A. D.; Weck, M.; Pine, D. J. Colloids with Valence and Specific Directional Bonding. *Nature* **2012**, 491, 51–55.
- (4) Choueiri, R. M.; Galati, E.; Thérien-Aubin, H.; Klinkova, A.; Larin, E. M.; Querejeta-Fernández, A.; Han, L.; Xin, H. L.; Gang, O.; Zhulina, E. B.; Rubinstein, M.; Kumacheva, E. Surface Patterning of Nanoparticles with Polymer Patches. *Nature* **2016**, 538, 79–83.
- (5) Gröschel, A. H.; Walther, A.; Löbling, T. I.; Schacher, F. H.; Schmalz, H.; Müller, A. H. E. Guided Hierarchical Co-assembly of Soft Patchy Nanoparticles. *Nature* **2013**, *503*, 247–251.
- (6) Walther, A.; Müller, A. H. E. Janus Particles: Synthesis, Self-Assembly, Physical Properties, and Applications. *Chem. Rev.* **2013**, 113, 5194–5261.
- (7) Wang, B. B.; Li, B.; Zhao, B.; Li, C. Y. Amphiphilic Janus Gold Nanoparticles via Combining "Solid State Grafting to" and "Grafting-from" Methods. J. Am. Chem. Soc. 2008, 130, 11594–11595.

- (8) Aveyard, R. Can Janus Particles Give Thermodynamically Stable Pickering Emulsions? *Soft Matter* **2012**, *8*, 5233–5240.
- (9) Liu, H.; Luo, J. C.; Shan, W. P.; Guo, D.; Wang, J.; Hsu, C.-H.; Huang, M. J.; Zhang, W.; Lotz, B.; Zhang, W.-B.; Liu, T. B.; Yue, K.; Cheng, S. Z. D. Manipulation of Self-Assembled Nanostructure Dimensions in Molecular Janus Particles. *ACS Nano* **2016**, *10*, 6585–6596.
- (10) Kim, J.; Song, X.; Kim, A.; Luo, B.; Smith, J. W.; Ou, Z.; Wu, Z.; Chen, Q. Reconfigurable Polymer Shells on Shape-Anisotropic Gold Nanoparticle Cores. *Macromol. Rapid Commun.* **2018**, 39, 1800101.
- (11) Galati, E.; Tao, H. C.; Tebbe, M.; Ansari, R.; Rubinstein, M.; Zhulina, E. B.; Kumacheva, E. Helicoidal Patterning of Nanorods with Polymer Ligands. *Angew. Chem., Int. Ed.* **2019**, *58*, 3123–3127.
- (12) Yu, L.; Shi, R.; Qian, H.-J.; Lu, Z.-Y. Versatile Fabrication of Patchy Nanoparticles via Patterning of Grafted Diblock Copolymers on NP Surface. *Phys. Chem. Chem. Phys.* **2019**, *21*, 1417–1427.
- (13) Zhou, Y. R.; Ma, X. D.; Zhang, L. S.; Lin, J. P. Directed Assembly of Functionalized Nanoparticles with Amphiphilic Diblock Copolymers. *Phys. Chem. Chem. Phys.* **2017**, *19*, 18757–18766.
- (14) Rossner, C.; Zhulina, E. B.; Kumacheva, E. Staged Surface Patterning and Self-Assembly of Nanoparticles Functionalized with End-Grafted Block Copolymer Ligands. *Angew. Chem., Int. Ed.* **2019**, 58, 9269–9274.
- (15) Yang, Y. Q.; Yi, C. L.; Duan, X. Z.; Wu, Q.; Zhang, Y.; Tao, J.; Dong, W. H.; Nie, Z. H. Block-Random Copolymer-Micellization-Mediated Formation of Polymeric Patches on Gold Nanoparticles. *J. Am. Chem. Soc.* **2021**, *143*, 5060–5070.
- (16) Yi, C. L.; Yang, Y. Q.; Nie, Z. H. Alternating Copolymerization of Inorganic Nanoparticles. *J. Am. Chem. Soc.* **2019**, *141*, 7917–7925. (17) Yi, C. L.; Liu, H.; Zhang, S. Y.; Yang, Y. Q.; Zhang, Y.; Lu, Z. Y.; Kumacheva, E.; Nie, Z. H. Self-Limiting Directional Nanoparticle Bonding Governed by Reaction Stoichiometry. *Science* **2020**, *369*, 1369–1374.
- (18) Rossner, C.; Tang, Q.; Müller, M.; Kothleitner, G. Phase Separation in Mixed Polymer Brushes on Nanoparticle Surfaces Enables the Generation of Anisotropic Nanoarchitectures. *Soft Matter* **2018**, *14*, 4551–4557.
- (19) Tao, H. C.; Chen, L. Y.; Galati, E.; Manion, J. G.; Seferos, D. S.; Zhulina, E. B.; Kumacheva, E. Helicoidal Patterning of Gold Nanorods by Phase Separation in Mixed Polymer Brushes. *Langmuir* **2019**, *35* (48), 15872–15879.
- (20) Zhang, N.; Yu, L.; Li, Y.-C.; Liu, H.; Lu, Z.-Y. Novel Nano-Patterned Structures of Mixed Hairy Nanoparticles in Single Layer. *Polymer* **2020**, *192*, 122295.
- (21) Roan, J.-R. Soft Nanopolyhedra as a Route to Multivalent Nanoparticles. *Phys. Rev. Lett.* **2006**, *96*, 248301.
- (22) Marko, J. F.; Witten, T. A. Phase Separation in a Grafted Polymer Layer. *Phys. Rev. Lett.* **1991**, *66*, 1541–1544.
- (23) Zhulina, E.; Balazs, A. C. Designing Patterned Surfaces by Grafting Y-Shaped Copolymers. *Macromolecules* **1996**, *29*, 2667–2673.
- (24) Sidorenko, A.; Minko, S.; Schenk-Meuser, K.; Duschner, H.; Stamm, M. Switching of Polymer Brushes. *Langmuir* **1999**, *15*, 8349–8355.
- (25) Minko, S.; Müller, M.; Usov, D.; Scholl, A.; Froeck, C.; Stamm, M. Lateral versus Perpendicular Segregation in Mixed Polymer Brushes. *Phys. Rev. Lett.* **2002**, *88*, 035502.
- (26) Zubarev, E. R.; Xu, J.; Sayyad, A.; Gibson, J. D. Amphiphilicity-Driven Organization of Nanoparticles into Discrete Assemblies. *J. Am. Chem. Soc.* **2006**, *128*, 15098–15099.
- (27) Zhao, B.; Zhu, L. Mixed Polymer Brush-Grafted Particles: A New Class of Environmentally Responsive Nanostructured Materials. *Macromolecules* **2009**, 42, 9369–9383.
- (28) Song, J. B.; Cheng, L.; Liu, A. P.; Yin, J.; Kuang, M.; Duan, H. W. Plasmonic Vesicles of Amphiphilic Gold Nanocrystals: Self-Assembly and External-Stimuli-Triggered Destruction. *J. Am. Chem. Soc.* **2011**, *133*, 10760–10763.

- (29) Guzman-Juarez, B.; Abdelaal, A.; Kim, K.; Toader, V.; Reven, L. Fabrication of Amphiphilic Nanoparticles via Mixed Homopolymer Brushes and NMR Characterization of Surface Phase Separation. *Macromolecules* **2018**, *51*, 9951–9960.
- (30) Wang, J.; Müller, M. Microphase Separation of Mixed Polymer Brushes: Dependence of the Morphology on Grafting Density, Composition, Chain-Length Asymmetry, Solvent Quality, and Selectivity. *J. Phys. Chem. B* **2009**, *113*, 11384–11402.
- (31) Wang, Y.; Yang, G.; Tang, P.; Qiu, F.; Yang, Y.; Zhu, L. Mixed Homopolymer Brushes Grafted Onto a Nanosphere. *J. Chem. Phys.* **2011**, *134*, 134903.
- (32) Chen, C.; Zhang, T.; Zhu, L.; Zhao, B.; Tang, P.; Qiu, F. Hierarchical Superstructures Assembled by Binary Hairy Nanoparticles. ACS Macro Lett. 2016, 5, 718–723.
- (33) Matyjaszewski, K.; Xia, J. Atom Transfer Radical Polymerization. Chem. Rev. 2001, 101, 2921–2990.
- (34) Hawker, C. J.; Bosman, A. W.; Harth, E. New Polymer Synthesis by Nitroxide Mediated Living Radical Polymerizations. *Chem. Rev.* **2001**, *101*, 3661–3688.
- (35) Li, D. J.; Sheng, X.; Zhao, B. Environmentally Responsive "Hairy" Nanoparticles: Mixed Homopolymer Brushes on Silica Nanoparticles Synthesized by Living Radical Polymerization Techniques. *J. Am. Chem. Soc.* **2005**, *127*, 6248–6256.
- (36) Bao, C. H.; Tang, S. D.; Wright, R. A. E.; Tang, P.; Qiu, F.; Zhu, L.; Zhao, B. Effect of Molecular Weight on Lateral Microphase Separation of Mixed Homopolymer Brushes Grafted on Silica Particles. *Macromolecules* **2014**, *47*, 6824–6835.
- (37) Chancellor, A. J.; Seymour, B. T.; Zhao, B. Characterizing Polymer-Grafted Nanoparticles: From Basic Defining Parameters to Behavior in Solvents and Self-Assembled Structures. *Anal. Chem.* **2019**, *91*, 6391–6402.
- (38) Hiemenz, P. C.; Lodge, T. P. Polymer Chemistry, 2nd ed.; CRC Press: Boca Raton, FL, 2007.
- (39) Horton, J. M.; Tang, S.; Bao, C.; Tang, P.; Qiu, F.; Zhu, L.; Zhao, B. Truncated Wedge-Shaped Nanostructures Formed from Lateral Microphase Separation of Mixed Homopolymer Brushes Grafted on 67 nm Silica Nanoparticles: Evidence of the Effect of Substrate Curvature. ACS Macro Lett. 2012, 1, 1061–1065.
- (40) Kim, S.; Kim, T.-H.; Huh, J.; Bang, J.; Choi, S.-H. Nanoscale Phase Behavior of Mixed Polymer Ligands on a Gold Nanoparticle Surface. *ACS Macro Lett.* **2015**, *4*, 417–421.
- (41) Tang, C.; Lennon, E. M.; Fredrickson, G. H.; Kramer, E. J.; Hawker, C. J. Evolution of Block Copolymer Lithography to Highly Ordered Square Arrays. *Science* **2008**, 322, 429–432.
- (42) Fox, T. L.; Tang, S. D.; Horton, J. M.; Holdaway, H. A.; Zhao, B.; Zhu, L.; Stewart, P. L. In-Situ Characterization of Binary Mixed Polymer Brush-Grafted Silica Nanoparticles in Aqueous and Organic Solvents by Cryo-Electron Tomography. *Langmuir* **2015**, *31*, 8680–8688
- (43) Soga, K. G.; Zuckermann, M. J.; Guo, H. Binary Polymer Brush in a Solvent. *Macromolecules* **1996**, 29, 1998–2005.